

SCIENTIFIC REPORTS



OPEN

Nonlinear inelastic electron scattering from Au nanostructures induced by localized surface plasmon resonance

ZheAn Li¹, ChunKai Xu^{1,2}, WenJie Liu¹, Meng Li¹ & XiangJun Chen^{1,2}

Nonlinear electron scattering is a recently-discovered physical process observed during the localized plasmonic excitation of Ag nanostructures on graphite surface. In the present work, nonlinear electron scattering phenomena is experimentally verified on Au nanostructures by measuring inelastic scattering of electrons field-emitted from tungsten tip. The relative intensity of the electron-energy-loss peak associated with the plasmonic excitation of Au shows again to increase nonlinearly with the electric field generated by the tip-sample bias, demonstrating the generality of nonlinear electron scattering process in plasmonic system. Compared to the nonlinear electron scattering phenomena observed on Ag nanostructures, the nonlinear term for Au nanostructures is about 1 to 2 orders of magnitude smaller, which is in consistent with the field enhancement factor of Au and Ag nanostructures from both the surface-enhanced Raman spectroscopy experiments and the theoretical calculations.

Scanning probe electron energy spectroscopy (SPEES) is an emerging technique which can obtain spectroscopy mapping of surface with spatial resolution^{1–8}. In this technique, the tip of a scanning tunnel microscope is operated in the field emission mode to generate a local electron beam, which can be scattered from the surface and collected by an electron energy analyzer. Therefore, the two dimensional distribution of the electron energy spectra of the surface can be scanned^{2,5,7,8}, which is important information for fully understanding the surface at microscale. However, the probability of the inelastic scattering of electron is usually very small, often orders of magnitude smaller than that of the elastically scattered electron. It thus becomes a bottleneck for improving the spatial resolution of this developing technique. This difficulty may be overcome by a recently-discovered new physical process, named nonlinear electron scattering, in which the intensity of the inelastic scattering electron signal can be nonlinearly enhanced to the same level of its elastic counterpart, during the excitation of the localized surface plasmon resonance (LSPR) on Ag nanostructures⁹. According to the theoretical explanation⁹, extremely high localized electric field is produced by the “hot spots” formed between Ag nanostructures and modulated by the external electric field, which consequently induces nonlinear electron scattering process. This is benefited from the large field enhancement factor of Ag nanostructures, as often demonstrated in the surface-enhanced Raman spectroscopy (SERS) experiments^{10–17}. On the other hand, Au nanostructure also has large field enhancement factor, which, in combination with its high chemical and physical stability, makes it being widely used in the panorama of nanoscience and nanotechnology^{18–20}. Therefore, it should be very interesting to investigate whether the large field enhancement factor of Au nanostructures can also lead to the nonlinear electron scattering phenomena.

In this article, we report the SPEES experiments carried out on Au nanostructures on graphite surface. It is observed that the relative intensity of the inelastic scattered electron due to the Au LSPR excitation increases nonlinearly with respect to the external electric field generated by the tip-sample bias, demonstrating the generality of the nonlinear electron scattering phenomena in plasmonic system during the electron scattering process. The observed nonlinear term for Au nanostructures is about 1 to 2 orders of magnitude smaller than that for Ag

¹Hefei National Laboratory for Physical Sciences at the Microscale and Department of Modern Physics, University of Science and Technology of China, Hefei, 230026, China. ²Synergetic Innovation Center of Quantum Information and Quantum Physics, University of Science and Technology of China, Hefei, 230026, China. Correspondence and requests for materials should be addressed to C.X. (email: xuck@ustc.edu.cn) or X.C. (email: xjun@ustc.edu.cn)

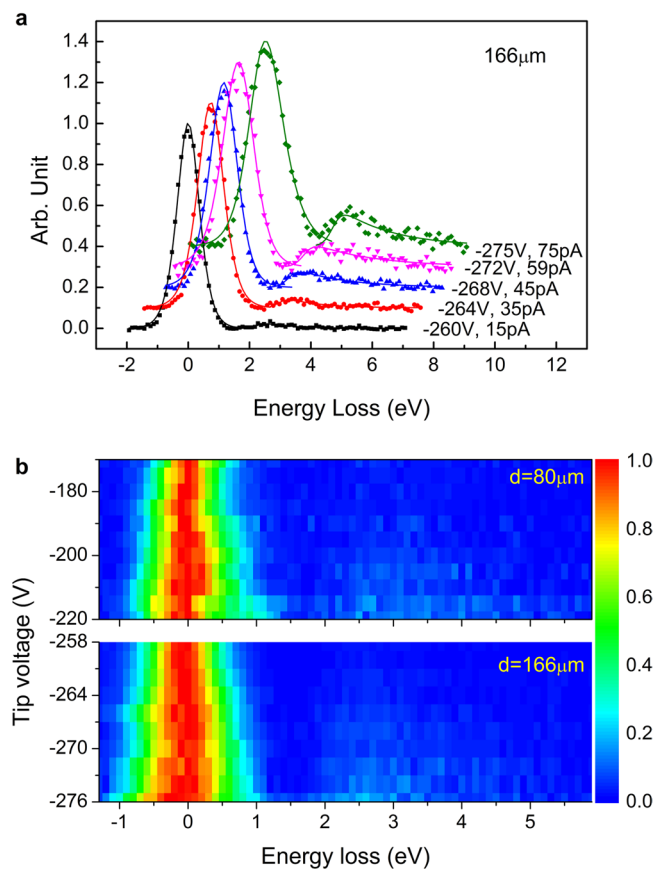


Figure 1. EELSs acquired at different tip voltages under different tip-sample distances. (a) EELSs acquired at tip-sample distance 166 μm with different tip voltages and sample currents. (b) Two dimensional plots of the measured electron scattering intensity as a function of energy loss and tip voltage at two different tip-sample distances. For comparison, all EELSs have been background-subtracted by polynomial function and divided by the amplitude of the elastic scattering peak.

nanostructures. This is in accordance with the field enhancement factor of Au and Ag nanostructures obtained by the SERS experiments^{21–24}, as well as the theoretical calculations²⁵.

Results

The experiments are carried out by a home-made scanning probe electron energy spectrometer, the detailed description of which can be found elsewhere⁵. Briefly, it consists of a tip-sample system and a toroidal electron energy analyzer (TEEA)²⁶. In the experiment, electrons field-emitted from a tungsten tip are used to excite the LSPR of Au nanostructures, which is prepared by evaporating 30 nm Au on HOPG surface. The scattered electrons are collected and analyzed by the TEEA (see Methods). Electron energy loss spectra (EELS) are obtained at two different tip-sample distances, 166 μm and 80 μm. At each distance, the tip voltage is increased step by step. As examples, EELS acquired at 166 μm with five different tip voltages are shown in Fig. 1(a), where the experimental data are denoted as scattered points and the fitted curves are plotted as solid lines. Each spectrum has been background-subtracted by polynomial function and normalized by the amplitude of the elastic scattering peak for comparison^{4,9}. The energy loss peak located at around 2.6 eV is attributed to the excitation of Au LSPR. Similar to the phenomena observed on Ag nanostructures⁹, the intensity of the LSPR peak in EELS obtained at relatively low tip voltage is very weak, whereas it is significantly enhanced when the tip voltage increases. The full data acquired at two different tip-sample distances are presented by two dimensional plots in Fig. 1(b), showing the electron scattering intensity as a function of energy loss and tip voltage. It can be seen that at both tip-sample distances, the intensity of the LSPR peak increases with the tip voltage.

Discussion

From the surface electronic excitation theory^{27–29}, we have the knowledge that surface plasmon is excited mainly through the long-range dipole scattering process. At backscattering condition in our experiments, the LSPR excitation must be a multiple-scattering process of a large-angle elastic scattering followed by a near-zero-angle dipole scattering. Therefore the transition probability of LSPR excitation can be obtained experimentally from the intensity ratio of the inelastic scattering peak to the elastic scattering peak in EELS, which is defined as the relative intensity (*RI*) in our previous work on Ag nanostructures⁹. Similarly, in this work we also obtain *RI* for Au nanostructures. Its dependence on tip voltage at each tip-sample distance is shown in Fig. 2. It is obvious that *RI*

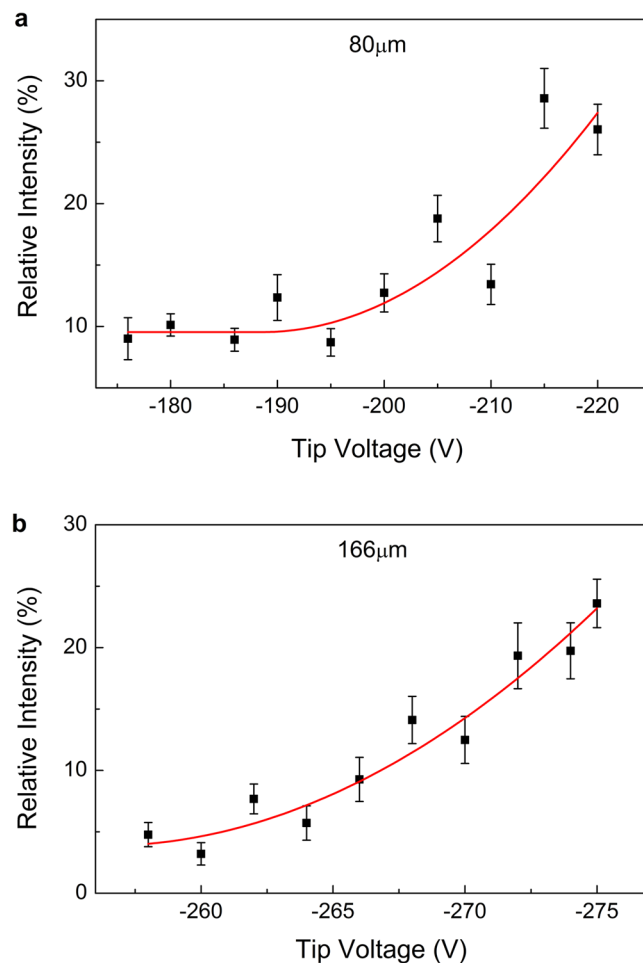


Figure 2. The dependence of the relative intensity (*RI*) on tip voltage under different tip-sample distances. **(a)** 80 μm. **(b)** 166 μm. The solid square with error bar represents calculated *RI* from the experimental data, and the solid lines are quadratic fitted curves.

increases nonlinearly with the tip voltage, demonstrating the occurrence of the nonlinear electron scattering process during the LSPR excitation on Au nanostructures. However, the *RI* increase rate with respect to tip voltage are smaller than that of Ag nanostructures, which should be attributed to the difference between the properties of the LSPR states for Au nanostructures and Ag nanostructures.

According to the theory proposed in ref.⁹, the transition probability W_{ba} of the LSPR excitation can be described by the perturbation theory considering the second-order interaction under the dipole approximation, and can be expressed as

$$W_{ba} = W_{ba}^{(1)} + W_{ba}^{(2)} \propto |\langle b | \vec{E}_1 \cdot \vec{D}_{ba} | a \rangle|^2 + \sum_n \left| \frac{\langle b | \vec{E}_2 \cdot \vec{D}_{bn} | n \rangle \langle n | \vec{E}_1 \cdot \vec{D}_{na} | a \rangle}{\Gamma_n/2} \right|^2 \quad (1)$$

Here $|a\rangle$ and $|b\rangle$ are the ground state and the excited LSPR state, and $|n\rangle$ is an intermediate state with energy width Γ_n . D_{ba} , D_{bn} and D_{na} are the matrix elements of the dipolar moment operator for electron scattering, \vec{E}_1 and \vec{E}_2 are the electric field experienced by $|a\rangle$ and $|n\rangle$, and the sum over n is over all possible intermediate states. In the conventional EELS experiments such as high resolution EELS (HREELS)^{29,30} and EELS in scanning transmission electron microscope (STEM-EELS)^{31–34}, the second-order term $W_{ba}^{(2)}$ is much smaller than the first-order term $W_{ba}^{(1)}$ and can be neglected, consequently the transition probability is dominated by the latter one and shows no dependence on the external field. However, in the nonlinear electron scattering phenomena observed in the present work on Au nanostructures as well as in the previous work on Ag nanostructures⁹, the probability of the LSPR excitation is largely enhanced, indicating that $W_{ba}^{(2)}$ should play an important role. From the electromagnetic mechanism in SERS experiments^{21–25}, we have the knowledge that noble metal nanostructure will enhance the incoming electric field by a large field enhancement factor f through LSPR, generating an extremely high localized electric field. The same mechanism can also be applied to electron scattering process, resulting in an enhanced local field when the LSPR of noble metal nanostructure is excited. According to the expression

	Au		Ag ⁹		
	80	166	92	114	150
tip-sample distances (μm)	80	166	92	114	150
nonlinear coefficient (μm ² /V ²)	1	15	166	67	83

Table 1. The nonlinear coefficient.

$$W_{ba}^{(2)} \propto \left| \frac{\langle b | \vec{E}_2 \cdot \vec{D}_{bn} | n \rangle \langle n | \vec{E}_1 \cdot \vec{D}_{na} | a \rangle}{\Gamma_n/2} \right|^2 \quad (2)$$

all intermediate states $|n\rangle$ can in principle contribute to $W_{ba}^{(2)}$. However, as described in ref.⁹, only the final state $|b\rangle$ will experience the enhanced field and thus contribute mostly to $W_{ba}^{(2)}$, which is then approximated to

$$W_{ba}^{(2)} \propto \left| \frac{\langle b | \vec{E}_2 \cdot \vec{D}_b | b \rangle \langle b | \vec{E}_1 \cdot \vec{D}_{ba} | a \rangle}{\Gamma_b/2} \right|^2 \propto \left(\frac{2\mu_b E_2}{\Gamma_b} \right)^2 W_{ba}^{(1)}. \quad (3)$$

Here μ_b and Γ_b are permanent dipole moment and energy width of the final state $|b\rangle$ respectively, and \vec{E}_2 is the enhanced localized electric field. This will lead to a significant LSPR peak in EELS, and the transition probability of LSPR, i.e. RI , should be quadratically dependent on the electric field, as clearly shown by our experimental observations on both Au nanostructures and Ag nanostructures. The coefficient of the quadratic term (can also be referred to nonlinear coefficient) should consequently be proportional to f^2 . Therefore, comparing the nonlinear coefficient of Au nanostructures with that of Ag nanostructures will provide information about the field enhancement factor for LSPR state, which is very important in the field of plasmonics and nanophotonics.

From the tip-sample distance and tip voltage, we can estimate the electric field, and the dependence of RI on electric field can be obtained. By fitting the data with a quadratic function, the nonlinear coefficient can be determined. The results for the two tip-sample distances of Au nanostructures are listed in Table 1. The nonlinear coefficients for Ag nanostructures at three different tip-sample distances are also determined from the previous nonlinear electron scattering experimental data⁹ and compiled in Table 1 for comparison.

It is clearly shown that the nonlinear coefficient for Au nanostructures is about 1 to 2 orders of magnitude smaller than that for Ag nanostructures. The field enhancement factor f for Ag and Au nanostructures has been studied intensively by both SERS experiments^{21–24} and theoretical calculations²⁵. Orendorff *et al.* measured the electromagnetic enhancement factor (EF) of SERS for Ag and Au nanostructures with average size about 30 nm²¹, which are quite similar to the samples we used in our experiment. By measuring SERS signal from 4-Mercaptopyridine molecules deposited on surface, the EFs for Ag and Au nanostructures are determined to be $4.8 \pm 0.5 \times 10^6$ and $1.2 \pm 0.2 \times 10^4$ respectively. Considering EF is proportional to f^{415} , their results are in good agreement with our measurements. On the other hand, Tanabe²⁵ directly calculated the field enhancement factors for Ag and Au nanoparticles, which is also in consistent with our experiments. From these comparisons, it is evidently confirmed that nonlinear electron scattering should be a general phenomenon existing in plasmonic system. The results also indicate that the nonlinear electron scattering is a potential method to study the properties of the LSPR states of noble metal nanostructures, which is very important but difficult to be investigated due to the ultra-short dumping time.

In summary, EELSs for Au nanostructures on HOPG surface have been measured by a home-made scanning probe electron energy spectrometer with different tip voltages at different tip-sample distances. It is shown that the relative intensity RI of the inelastic scattering electron due to Au LSPR excitation increases nonlinearly with the electric field, demonstrating the generality of nonlinear electron scattering process in plasmonic system. Compared to the previous nonlinear electron scattering work on Ag nanostructures, the nonlinear coefficient for Au nanostructures is about 1 to 2 orders of magnitude smaller, which is in consistent with previous studies on field enhancement factors for Au and Ag nanostructures by both SERS experiments and theoretical calculations.

As we have mentioned in our last paper⁹, the observation of nonlinear electron scattering lays the foundation for a new spectroscopic technology, namely nonlinear electron scattering spectroscopy (NESS). The confirmation of the generality of the nonlinear electron scattering phenomenon in this work further augments the possibility of this potential technology. Due to the high chemical and physical stability of Au, it would be more proper to employ Au nanostructures as the substrate in NESS technology to generate localized electric “hot spot”, which will act as a highly confined ultra-fast laser source^{35,36} to excite the adsorbates and consequently high spatial and spectral resolution will be acquired.

Methods

Experimental setup. The experiments are carried out by a home-made scanning probe electron energy spectrometer, detailed description of which can be found elsewhere⁵. Briefly, it consists of a tip-sample system and a toroidal electron energy analyzer (TEEA)²⁶, and is capable of acquiring EELS under a close tip-sample distance with different tip voltages. The geometry of the experiment is illustrated in Fig. 3a, while Fig. 3b shows the enlarged part of the tip-sample area. In the experiment, a tip made from a 0.42 mm tungsten wire by electrochemical etching was approached to a distance of micrometers from the grounded sample surface, which was prepared by evaporating 30 nm thin film of Au on freshly cleaved HOPG. The topography image of the sample surface is

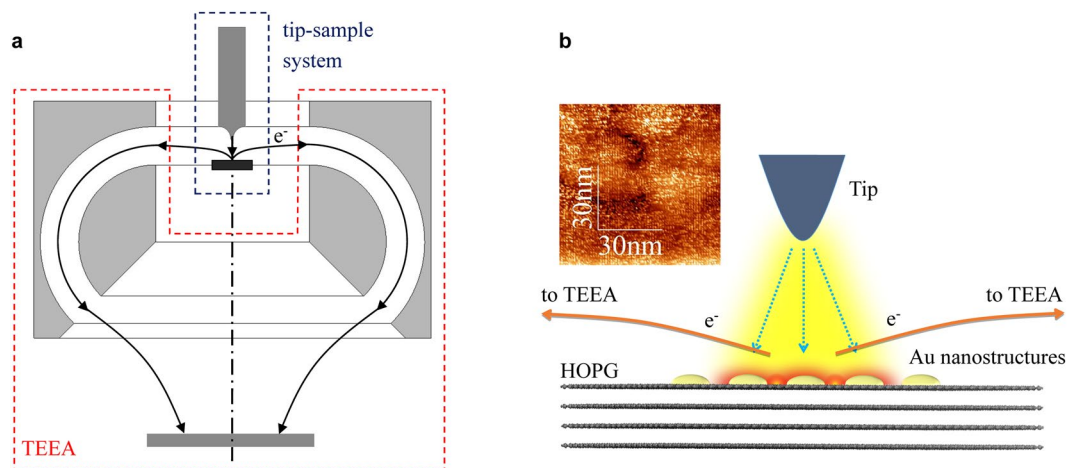


Figure 3. The experimental arrangement. **(a)** The sketch of the spectrometer which consists of a tip-sample system and a toroidal electron energy analyzer (TEEA). **(b)** The enlarged part of the tip-sample area. A tungsten tip is approached to a distance of micrometers from the sample surface, which is prepared by evaporating about 30 nm thick Au on HOPG. Au nanostructures can be observed in the topography image as shown in the inset. A negative voltage of hundred volts is applied to the tip while keep the sample surface grounded to produce field-emission electrons. The localized surface plasmon resonance of the Au nanostructures is excited by the field-emission electrons and the backscattered electrons are collected and energy-analyzed by a TEEA.

shown in the inset of Fig. 3b, where Au nanostructures can be observed. A negative voltage V_t of hundred volts was then applied to the tip to generate field-emission electrons to impact perpendicularly with the sample surface. According to the geometry of the spectrometer shown in Fig. 3a, the backscattered electrons outgoing parallel to the sample surface were collected and analyzed by the TEEA. In this way the EELS under a certain tip-sample distance and tip bias was acquired. In the present work, the experiments were performed at two tip-sample distances, 166 μm and 80 μm .

Data analysis. For each EELS, firstly the background-subtraction by polynomial function was performed. Then we deconvoluted the elastic scattering (ES) peak and the LSPR excitation peak in EELS, and calculate the RI by dividing the LSPR peak area with ES peak area. By increasing the tip voltage step by step while keeping the tip-sample distance unchanged, the EELSs at different electric field were obtained, and consequently the corresponding RI s were calculated.

Data availability. The data that support the findings of this study are available from the corresponding author (C.K.X.) upon reasonable request.

References

- Eves, B. J., Festy, F., Svensson, K. & Palmer, R. E. Scanning probe energy loss spectroscopy: angular resolved measurements on silicon and graphite surfaces. *App. Phys. Lett.* **77**, 4223–4225 (2000).
- Festy, F. & Palmer, R. E. Scanning probe energy loss spectroscopy below 50 nm resolution. *App. Phys. Lett.* **85**, 5034–5036 (2004).
- Yin, J. L., Pulisciano, A. & Palmer, R. E. Local Secondary-electron emission spectra via scanning probe energy loss spectroscopy. *Small* **2**, 744–746 (2006).
- Pulisciano, A., Park, S. J. & Palmer, R. E. Surface plasmon excitation of Au and Ag in scanning probe energy loss spectroscopy. *Appl. Phys. Lett.* **93**, 213109 (2008).
- Xu, C. K. *et al.* Spatially resolved scanning probe electron energy spectroscopy for Ag islands on a graphite surface. *Rev. Sci. Instrum.* **80**, 103705 (2009).
- Song, M. Y., Lawton, J. J., Robinson, A. P. G. & Palmer, R. E. Scanning probe energy loss spectroscopy with microfabricated coaxial tips. *Phys. Rev. B* **81**, 161411(R) (2010).
- Murphy, S. *et al.* Mapping the plasmon response of Ag nanoislands on graphite at 100 nm resolution with scanning probe energy loss spectroscopy. *Appl. Phys. Express* **8**, 126601 (2015).
- Li, M. *et al.* Electron energy spectroscopy mapping of surface with scanning tunneling microscope. *Rev. Sci. Instrum.* **87**, 086108 (2016).
- Xu, C. K. *et al.* Nonlinear inelastic electron scattering revealed by plasmon-enhanced electron energy-loss spectroscopy. *Nature Phys.* **10**, 753–757 (2014).
- Nie, S. & Emory, S. R. Probing single molecules and single nanoparticles by surface-enhanced Raman scattering. *Science* **275**, 1102–1106 (1997).
- Kneipp, K. *et al.* Single molecule detection using surface-enhanced Raman scattering (SERS). *Phys. Rev. Lett.* **78**, 1667–1670 (1997).
- Willems, K. A. & Van Duyne, R. P. Localized surface plasmon resonance spectroscopy and sensing. *Annu. Rev. Phys. Chem.* **58**, 267–297 (2007).
- Cang, H. *et al.* Probing the electromagnetic field of a 15-nanometre hotspot by single molecule imaging. *Nature* **469**, 385–388 (2011).
- Sharma, B. *et al.* SERS: materials, applications, and the future. *Mater. Today* **15**, 16–25 (2012).
- González, P. A. *et al.* Resolving the electromagnetic mechanism of surface-enhanced light scattering at single hot spots. *Nature Commun.* **3**, 684 (2012).
- Zhang, R. *et al.* Chemical mapping of a single molecule by plasmon-enhanced Raman scattering. *Nature* **498**, 82–86 (2013).

17. Gruenke, N. L. *et al.* Ultrafast and nonlinear surface-enhanced Raman spectroscopy. *Chem. Soc. Rev.* **45**, 2263–2290 (2016).
18. Daniel, M. C. & Astruc, D. Gold nanoparticles: Assembly, supramolecular chemistry, quantum-size-related properties, and applications toward biology, catalysis, and nanotechnology. *Chem. Rev.* **104**, 293–346 (2004).
19. Grigorenko, A., Roberts, N., Dickinson, M. & Zhang, Y. Nanometric optical tweezers based on nanostructured substrates. *Nature Photon.* **2**, 365–370 (2008).
20. Amendola, V. *et al.* Surface plasmon resonance in gold nanoparticles: a review. *J. Phys.: Condens. Matter* **29**, 203002 (2017).
21. Orendorff, C. J., Gearheart, L., Jana, N. R. & Murphy, C. J. Aspect ratio dependence on surface enhanced Raman scattering using silver and gold nanorod substrates. *Phys. Chem. Chem. Phys.* **8**, 165–170 (2006).
22. Strobbia, P., Languirand, E. & Cullum, B. M. Recent advances in plasmonic nanostructures for sensing: a review. *Opt. Eng.* **54**, 100902 (2015).
23. Yuan, H. K. *et al.* Spectral characterization and intracellular detection of surface-enhanced Raman scattering (SERS)-encoded plasmonic gold nanostars. *J. Raman Spectrosc.* **44**, 234–239 (2013).
24. Kneipp, K. *et al.* Extremely large enhancement factors in surface enhanced Raman scattering for molecules on colloidal gold clusters. *Appl. Spectrosc.* **52**, 1493–1497 (1998).
25. Tanabe, K. Field enhancement around metal nanoparticles and nanoshells: a systematic investigation. *J. Phys. Chem. C* **112**, 15721–15728 (2008).
26. Zhou, X. *et al.* Angle and energy dispersive multichannel electron energy spectrometer for surface analysis. *J. Electron Spectrosc. Relat. Phenom.* **165**, 15–19 (2008).
27. Lucas, A. A. & Šunjić, M. Fast-electron spectroscopy of surface excitations. *Phys. Rev. Lett.* **26**, 229–232 (1971).
28. Hall, B. M. & Mills, D. L. Excitation of surface plasmons on metals by low-energy electrons: The role of interference effects. *Phys. Rev. B* **44**, 1202–1208 (1991).
29. Rocca, M. Low-energy EELS investigation of surface electronic excitations on metals. *Surf. Sci. Rep.* **22**, 1–71 (1995).
30. Park, S. J. & Palmer, R. E. Acoustic plasmon on the Au(111) surface. *Phys. Rev. Lett.* **105**, 016801 (2010).
31. Nelayah, J. *et al.* Mapping surface plasmons on a single metallic nanoparticle. *Nature Phys.* **3**, 348–353 (2007).
32. Chu, M. W. *et al.* Probing bright and dark surface-plasmon modes in individual and coupled noble metal nanoparticles using an electron beam. *Nano Lett.* **9**, 399–404 (2009).
33. Koh, A. L. *et al.* Electron energy-loss spectroscopy (EELS) of surface plasmons in single silver nanoparticles and dimers: influence of beam damage and mapping of dark modes. *ACS Nano* **3**, 3015–3022 (2009).
34. Nicoletti, O. *et al.* Three-dimensional imaging of localized surface plasmon resonances of metal nanoparticles. *Nature* **502**, 80–84 (2013).
35. Dong, Z. C. *et al.* Generation of molecular hot electroluminescence by resonant nanocavity plasmons. *Nature Photon.* **4**, 50–54 (2010).
36. Tian, G., Liu, J. C. & Luo, Y. Density-matrix approach for the electroluminescence of molecules in a scanning tunneling microscope. *Phys. Rev. Lett.* **106**, 177401 (2011).

Acknowledgements

This work was partly supported by National Key Research and Development Program of China (Grant No. 2017YFA0303500) and National Natural Science Foundation of China (Grant Nos. 11674302).

Author Contributions

X.J.C. initiated the study. C.K.X. and X.J.C. supervised the project and designed experiments. C.K.X., W.J.L. and M.L. performed experiments. Z.A.L. analyzed the data. C.K.X., X.J.C. and Z.A.L. interpreted experiments and wrote the manuscript.

Additional Information

Competing Interests: The authors declare no competing interests.

Publisher's note: Springer Nature remains neutral with regard to jurisdictional claims in published maps and institutional affiliations.



Open Access This article is licensed under a Creative Commons Attribution 4.0 International License, which permits use, sharing, adaptation, distribution and reproduction in any medium or format, as long as you give appropriate credit to the original author(s) and the source, provide a link to the Creative Commons license, and indicate if changes were made. The images or other third party material in this article are included in the article's Creative Commons license, unless indicated otherwise in a credit line to the material. If material is not included in the article's Creative Commons license and your intended use is not permitted by statutory regulation or exceeds the permitted use, you will need to obtain permission directly from the copyright holder. To view a copy of this license, visit <http://creativecommons.org/licenses/by/4.0/>.

© The Author(s) 2018